A Novel Inhibitor of Signal Transducers And Activators Of Transcription 3 Activation Is Efficacious Against Established Central Nervous System Melanoma and Inhibits Regulatory T Cells

Ling-Yuan Kong,[1] Mohamed K. Abou-Ghazal,[1] Jun Wei,[1] Arup Chakraborty,[2] Wei Sun,[1] Wei Qiao,[3] Gregory N. Fuller,[4] Izabela Fokt,[2] Elizabeth A. Grimm,[5] Robert J. Schmittling,[6] Gary E. Archer, Jr.,[6] John H. Sampson,[6] Waldemar Priebe,[2] and Amy B. Heimberger[1]

Abstract

Purpose: Activation of signal transducers and activators of transcription 3 (STAT3) has been identified as a central mediator of melanoma growth and metastasis. We hypothesized that WP1066, a novel STAT3 blockade agent, has marked antitumor activity, even against the melanoma metastasis to brain, a site typically refractory to therapies.

Experimental Design: The antitumor activities and related mechanisms of WP1066 were investigated both *in vitro* on melanoma cell lines and *in vivo* on mice with subcutaneously syngeneic melanoma or with intracerebral melanoma tumors.

Results: WP1066 achieved an IC_{50} of 1.6, 2.3, and 1.5 μmol/L against melanoma cell line A375, B16, and B16EGFRvIII, respectively. WP1066 suppressed the phosphorylation of Janus-activated kinase 2 and STAT3 (Tyr705) in these cells. Tumor growth in mice with subcutaneously established syngeneic melanoma was markedly inhibited by WP1066 compared with that in controls. Long-term survival (>78 days) was observed in 80% of mice with established intracerebral syngeneic melanoma treated with 40 mg/kg of WP1066 in contrast to control mice who survived for a median of 15 days. Although WP1066 did not induce immunologic memory or enhance humoral responses to EGFRvIII, this compound reduced the production of immunosuppressive cytokines and chemokines (transforming growth factor-β, RANTES, MCP-1, vascular endothelial growth factor), markedly inhibited natural and inducible Treg proliferation, and significantly increased cytotoxic immune responses of T cells.

Conclusions: The antitumor cytotoxic effects of WP1066 and its ability to induce antitumor immune responses suggest that this compound has potential for the effective treatment of melanoma metastatic to brain.

Melanoma is a common and deadly tumor that despite the development of new therapeutic strategies, upon metastasis to the brain, is associated with a median survival time of <1 year. Furthermore, stage IV patients with brain metastasis are almost always excluded from participation in clinical trials. The Janus kinases (JAK)/signal transducers and activators of transcription (STAT)3 pathway is one of the key signaling pathways that drives the fundamental components of melanoma malignancy. The STAT3 protein is overexpressed in most cancers, including melanoma, and fosters tumorigenesis by preventing apoptosis (increases levels of the antiapoptotic proteins survivin, BCL-XL, and MCL1), enhancing proliferation (increases c-Myc and cyclin D1/D2 levels), angiogenesis [increases levels of vascular endothelial growth factor (VEGF) and hypoxia inducible factor], invasiveness (increases levels of matrix metalloproteinase 2 and matrix metalloproteinase 9), and metastasis (1, 2). Xie et al. (3) have shown that only highly metastatic melanoma cell lines, rather than poorly metastatic subtypes, overexpress matrix metalloproteinase 2, and have elevated levels of activated STAT3. Furthermore, blockade of activated STAT3 through expression of a dominant-negative STAT3 significantly suppresses invasiveness of the tumor cells, inhibits tumor growth, and prevents metastasis in nude mice. These studies indicate that STAT3 activation might be the crucial event in the development of melanoma metastasis.

STAT3 in the JAK/STAT pathway transduces extracellular signals such as cytokines and growth factors. The EGF receptor (EGFR) and interleukin 6 activate JAK, which subsequently activates STAT by phosphorylation of the tyrosine residue in

Authors' Affiliations: Departments of [1]Neurosurgery, [2]Experimental Therapeutics, [3]Biostatistics, [4]Pathology, and [5]Melanoma, The University of Texas M. D. Anderson Cancer Center, Houston, Texas and the [6]Division of Neurosurgery, Duke University Medical Center

Received 2/12/08; revised 6/4/08; accepted 6/5/08.

Grant support: The Anthony Bullock III Foundation, the Rose Foundation, the University of Texas M. D. Anderson Cancer Center, the NIH grants CA120813-01 and A1077225-01 (all to A.B. Heimberger) and by the University of Texas M. D. Anderson Cancer Center SPORE in melanoma P50 grant CA093459 (W. Priebe).

The costs of publication of this article were defrayed in part by the payment of page charges. This article must therefore be hereby marked *advertisement* in accordance with 18 U.S.C. Section 1734 solely to indicate this fact.

Note: W. Priebe and A.B. Heimberger are cosenior authors.

Requests for reprints: Amy B. Heimberger, Department of Neurosurgery, The University of Texas M. D. Anderson Cancer Center, Unit 442, 1515 Holcombe Boulevard, Houston TX 77030-4009. Phone: 713-792-2400; Fax: 713-794-4950; E-mail: aheimber@mdanderson.org.

doi:10.1158/1078-0432.CCR-08-0377

Translational Relevance

Development of new, effective therapies for metastatic melanoma that target novel pathways associated with the genesis of metastatic disease is a major unmet clinical need. Constitutive activation of STAT3 has been shown in a variety of human malignancies, including melanoma. We have designed and synthesized a series of potential inhibitors of the Janus-activated kinase/STAT3 pathway and identified a lead compound, WP1066, displaying high activity within *in vivo* models. In the study described here, we tested WP1066 in murine models of established central nervous system melanoma, a site typically refractory to therapies, and showed marked *in vitro* and *in vivo* activity. A key mechanism of activity of WP1066 includes the enhancement of cytotoxic T-cell responses and inhibition of regulatory T cells. Based on these preclinical data, WP1066 has therapeutic potential for the treatment of melanoma including intracerebral metastasis and as an immune therapy.

its transactivation domain. The EGF variant III (EGFRvIII) is constitutively active, with a cytoplasmic domain identical to that of the wild-type EGFR. The EGFR has been shown to physically interact with STAT3 (4, 5), and the phosphorylation of STAT3 has been attributed exclusively to EGFRvIII (6, 7), although this is controversial (8).

WP1066, a novel low molecular weight agent, has been shown to effectively block constitutively activated STAT3, JAK2/STAT3 activation by cytokines, and STAT5 (9–14) and to induce c-Myc degradation in multiple hematologic tumor cell types (15, 16). A recent study showed that treatment with WP1066 effectively inhibited the STAT3 pathway in glioma cell lines (U87-MG and U373-MG), down-regulated the antiapoptotic targets of STAT3 (BCL-XL, MCL-1, and c-Myc), and activated BCL2-associated X protein. WP1066 was found to increase the percentage of glioma cells undergoing apoptosis in a dose-dependent manner. Furthermore, in a murine subcutaneous model of malignant glioma, mice repeatedly injected i.p. with WP1066 (40 mg/kg) showed a significant inhibition in the growth of the tumors generated from U87-MG cells (12).

STAT3 has recently been hypothesized to be a key regulator of immunosuppression in cancer patients and is therefore considered a potential target for immunotherapy (17, 18). A pharmacologic agent capable of achieving physiologically relevant central nervous system (CNS) concentrations that is also able to restore or improve the immune responses of patients while exerting direct tumor cytotoxicity, would be highly desirable. We have recently shown that WP1066 can penetrate the CNS in mice and, in physiologically relevant doses *in vitro*, reverse tolerance in immune cells isolated from glioblastoma multiforme patients (19). WP1066 activates the immune system by inducing expression of costimulatory molecules, stimulating the production of the immune-stimulatory cytokines, and inducing T-cell effector responses, even in cancer patients who are refractory to the CD3 stimulation (19). The immune activation induced by WP1066 correlated with the phosphorylation of the respective tyrosine kinases Syk (Tyr352) in monocytes and ZAP-70 (Tyr319) in T cells. The combination of antitumor cytotoxic effects, the induction of antitumor immune responses, easy oral administration, and excellent CNS penetration provided compelling rationale for testing WP1066 against a variety of cancers, but especially against melanoma, which is dependent on STAT3, has been frequently targeted with immunotherapy (20), and frequently involves the CNS.

Materials and Methods

Tumor cell lines and murine models. The B16/F10 murine melanoma cell line was derived from a spontaneous melanoma in the C57BL/6J mouse of the H-2B background and was provided by Dr. Isaiah Fidler [The University of Texas M. D. Anderson Cancer Center (M. D. Anderson), Houston, TX]. The B16 cell line was stably transfected with the mouse EGFRvIII (kindly provided by Dr. Darrell Bigner of Duke University Medical Center, Durham, NC) to produce B16EGFRvIII cells, which provide an immunologic target for assessment of antigen-specific induced immune responses (21). The EGFRvIII expressed in these B16 cells is the murine equivalent of the human form of the receptor and is syngeneic within the B16/F10 model system. A375 is a human melanoma cell line that was provided by Dr. Elizabeth Grimm (M. D. Anderson, Houston, TX). The B16EGFRvIII cells were grown in Improved MEM Zinc Option medium (Life Technologies Bethesda Research Laboratories/Invitrogen) containing 10% fetal bovine serum. The B16 and A375 cell lines were maintained in RPMI 1640 supplemented with 10% fetal bovine serum at 37°C in a humidified atmosphere of 5% CO_2 and 95% air. All cell lines were grown in antibiotic-free medium and were free of *Mycoplasma* contamination (22).

For the *in vivo* experiments, we used 4- to 6-wk-old female C57BL/6J mice strictly inbred at M. D. Anderson and maintained in the M. D. Anderson Isolation Facility in accordance with Laboratory Animal Resources Commission standards and conducted according to an approved protocol, 08-06-11831.

Cell proliferation/survival assay. For cell proliferation assays, A375, B16, or B16EGFRvIII cells were seeded at a density of 2,000 cells per well in 96-well culture plates and were treated with WP1066 at increasing concentrations of 0, 0.155, 0.3125, 0.625, 1.25, 2.5, 5.0, and 10 μmol/L. After 72 h of treatment, 25 mL of 5 mg/mL dimethyl thiazolyl diphenyl tetrazolium salt (Sigma-Aldrich) solution were added to each well, and the cells were cultured for 3 h at 37°C in a humidified atmosphere of 5% CO_2 and 95% air. The cells were lysed with 100 μL per well of lysing buffer [50% dimethylformamide, 20% SDS (pH 5.6)] and incubated at room temperature overnight. Cell proliferation and viability were evaluated by reading the absorbance at 570 nm, and the IC_{50} was calculated.

Immunoprecipitation and immunoblotting analysis. Cells were rinsed with ice-cold PBS and lysed in cell culture plates for 30 min in ice-cold lysis buffer [50 mmol/L Tris-HCl (pH 8.0), 150 mmol/L NaCl, 1 mmol/L EDTA, 1% Triton-X-100, 1 mmol/L phenylmethylsulfonyl fluoride, 10 μg/mL leupeptin, 10 μg/mL aprotinin, and 1 mmol/L sodium vanadate]. The lysates were centrifuged at 14,000 rpm for 10 min at 4°C. The supernatants were collected and quantified for protein content. Equal amounts of proteins were electrophoretically fractionated in 8% SDS-polyacrylamide gels, transferred to nitrocellulose membranes, and subjected to immunoblot analysis with specific antibodies against phospho-STAT3 (Tyr705), total STAT3, c-Myc, phospho-AKT (Ser473), survivin (Cell Signaling Technology, Inc.), and β-actin (Sigma-Aldrich), respectively. In addition, the transferred membranes from B16 and B16EGFRvIII cell lysates were immunoblotted with a specific antibody against EGFRvIII (from Dr. Darrell Bigner, Duke University Medical Center, Durham, NC). Autoradiography of the membranes was done using Amersham enhanced chemiluminescence Western blotting detection reagents (Amersham Biosciences). For immunoprecipitation and immunoblotting analysis of phospho-JAK2, antiphosphotyrosine 4G10 (Upstate Biotechnology, Inc.) conjugated to agarose beads was used for immunoprecipitation, and anti-JAK2 antibody (Cell Signaling Technology, Inc.) was used for Western blotting.

In vivo *antitumor activity*. To induce the subcutaneous tumors, logarithmically growing B16EGFRvIII cells were injected into the right hind flank of C57BL/6J mice at a dose of 1.0×10^4 cells suspended in 100 μL of PBS. Tumors were measured every other day. Mice showing signs of morbidity were immediately euthanized according to the M. D. Anderson guidelines. Tumor volume was calculated with slide calipers using the following formula: $V = (L \times W \times H)/2$, where V is volume (mm^3), L is the long diameter, W is the short diameter, and H is the height.

To induce intracerebral tumors in C57BL/6J mice, B16 or B16EGFRvIII cells were collected in logarithmic growth phase, washed twice with PBS, mixed with an equal volume of 10% methyl cellulose in Improved MEM Zinc Option medium, and loaded into a 250-μL syringe (Hamilton) with an attached 25-gauge needle. The needle was positioned 2 mm to the right of bregma and 4 mm below the surface of the skull at the coronal suture using a stereotactic frame (Kopf Instruments). The intracerebral tumorigenic dose for the B16 or B16EGFRvIII cells was 5×10^2 in a total volume of 5 μL. Tumor rechallenge was done on mice surviving beyond 78 d (long-term survivors) by using the same cell dose and implantation coordinates in the contralateral hemisphere. Control naïve mice were challenged at the same time to verify the viability of the tumor rechallenge.

WP1066 was synthesized and supplied by a co-author (W.P.). It was dissolved in a mixture of 20 parts DMSO to 80 parts polyethylene glycol 300 (Sigma-Aldrich) at titered concentrations and delivered in a final volume of 100 μL. Before use, WP1066 was stored as a lyophilized powder at 4°C. Treatment was started 16 d after establishment of subcutaneous tumors and 3 d after intracerebral implantation, with titered doses of WP1066 injected i.p. or by oral gavage (o.g.) in a vehicle of DMSO/polyethylene glycol 300 (20 parts/80 parts) on a once per day schedule (5 d on, 2 d off). Ten mice per experimental group were used, including treatement with the DMSO/polyethylene glycol 300 vehicle alone in the control group.

Toxicity. Toxicity to female C57BL/6J mice was monitored by weighing them every other day, performing daily neurologic examinations on them consisting of monitoring stepping and placing reflexes, and histologic examination of the brain and systemic organs. The brain and systemic organs were assessed by immunohistochemistry and evaluated in a blinded fashion relative to treatment groups by subspecialty pathologists at the M. D. Anderson.

Quantification of cytokines and chemokines. B16 and B16EGFRvIII cells were seeded in 6-well culture plates at a density of 2×10^5 in 2 mL of complete cell culture medium per well and incubated overnight at 37°C. The next day, cells were treated with WP1066 at titered concentrations and incubated for 24 h at 37°C in a humidified atmosphere containing 5% CO_2 and 95% air. Supernatants were then collected and stored at -20°C for the measurement of TGF-β1 and VEGF concentrations using ELISA kits according to the manufacturer's instructions (R&D Systems). Briefly, the latent transforming growth factor (TGF)-β1 in the supernatants was first activated and neutralized to make it detectable by the immunoassay and then added in duplicate to precoated culture plates and incubated for 2 h at room temperature. After washing, horseradish peroxidase–conjugated detection antibody was added to each well and culture plates were incubated for another 2 h at room temperature. Finally, tetramethylbenzidine was added as substrate for color development. The absorbance was measured at 450 nm with a microplate reader (Spectra Max 190; Molecular Devices), and TGF-β1 and VEGF concentrations were quantified with the SoftMax Pro software (Molecular Devices). The detection limit for TGF-β1 ranged from 1.7 to 15.4 pg/mL and, for VEGF, from 125 to 2,000 pg/mL, with a lower limit of detection of 5 pg/mL. Concentrations of MCP-1 and RANTES were determined with multiplexed ELISA done by Quansys Biosciences (Quansys Biosciences). The detection limit for MCP-1 ranged from 15.6 to 1,000 pg/mL and, for RANTES, from 6.3 to 400 pg/mL.

EGFRvIII-specific humoral responses. Serum was obtained from the mice and stored at -20°C before analysis in a PEP-3-Dynabead assay. PEP-3, the 14-mer peptide that spans the mutated splice junction of EGFRvIII, was covalently linked to magnetic microspheres according to the manufacturer's instructions (Invitrogen). Briefly, the Dynabeads were incubated overnight in borate buffer (pH 9.5) with PEP-3 at 37°C on an end-over-end mixer. The following day, Dynabeads were washed and incubated an additional 2 h at 37°C in 0.1 mol/L Tris (pH 9) to further block any active sites. The final product was adjusted to 2×10^8 beads per mL with PBS + 0.1% bovine serum albumin + 0.25% sodium azide and stored at 2°C to 8°C.

Approximately 1×10^5 PEP-3 Dynabeads were added to the serum samples and incubated on a vortex mixer for 30 min at room temperature. Dynabeads were washed and further incubated with phycoerythrin-labeled goat-anti-mouse (1:100) for an additional 30 min. After washing away excess goat-anti-human-phycoerythrin, the Dynabeads were analyzed on a flow cytometer. All serum samples were initially diluted 1:100 with PBS + 0.1% Tween 20 and assayed in triplicate. To determine specificity, an additional sample set was preincubated for 15 min with 500 ng of the PEP-3 peptide to block any anti–PEP-3 that would be captured by the PEP-3–conjugated Dynabeads. The same criteria were used to establish equivalent binding units per milliliter (relative to nanogram of an anti-EGFRvIII monoclonal antibody L8A4 per milliliter) as previously described for human serum samples (23). The mean fluorescence intensit had to be at least 3.12, and the signal had to be at least 15% blocked by preincubation with free PEP-3. If the results met these criteria, the estimated binding

Table 1. Systemic histopathologic effects of WP1066 in C57BL/6 mice

Drug	Administration Route	Total (mg/kg)	Pathology of systemic organs							
			Spleen	Thymus	Lung	Heart	Kidney	Brain	Liver	GI
Vehicle	i.p.	N/A	1/10*, 2/10 †	0/8	0/9	0/10	0/10	0/10	1/10	4/10 ‡
WP1066	i.p.	20	4/5 †	0/7	1/7*	1/7§	2/7*	0/7	4/7*	1/6*, 2/6 ‡
WP1066	i.p.	10	4/10 †	0/8	1/10 † ‖	1/10*	3/10*	0/10	1/10¶, 2/10*	1/9*, 1/9 ‡
Vehicle	o.g.	N/A	3/10 †	1/8*	0/10	0/10	0/10	0/10	0/10	1/10*
WP1066	o.g.	40	0/5	0/5	0/5	0/4	1/5	0/5	1/5**,2/5*	0/4

Abbreviation: N/A, not applicable.
*Autolysis.
†Hemosiderin staining within macrophages.
‡Reactive lymphoid follicles with germinal center.
§Likely postmortem bacterial endocarditis.
‖Pulmonary congestion.
¶Chronic inflammatory infiltrate in connective tissue adjacent to the liver.
**Chronic inflammation.

units were extracted from the L8A4 standard curve. Standards of mouse anti–PEP-3 antibody (L8A4 per milliliter) were run with each assay and negative (normal serum) controls. The cytometer was standardized each day with phycoerythrin–fluorescence-activated cell sorting microbeads and unreacted PEP-3 Dynabeads.

Ex vivo *T-cell cytotoxicity assays*. Groups of nontumor-bearing animals were vaccinated with 100 μg of PEP-3-keyhole limpet hemocyanin (KLH) in a 1:1 ratio with complete Freund's adjuvant (CFA), 100 μg of PEP-3-KLH, 40 mg/kg of WP1066, or 100 μg of PEP-3-KLH with 40 mg/kg of WP1066, every 2 wk, for a total of 4 doses. Other than WP1066 (o.g.), the vaccinations were administered to the base of the tail, right groin, left groin, and flank, respectively. Standard assays were used to determine the percentage of cytolysis of the B16EGFRvIII cells by splenocytes obtained from C57BL/6J mice 48 h after the last vaccination (22). Splenocytes obtained from naïve C57BL/6J mice were used as negative controls.

Regulatory T-cell suppression assays. Single-cell suspensions were prepared from pooled lymph nodes and spleens of C57BL/6J mice. The CD4+ cells were enriched using CD4 MACS beads (Miltenyi Biotec) and were stained with peridinin-chlorophyll-protein complex–labeled anti-CD4 (L3T4), FITC-labeled anti-CD62L (MEL-14), and allophycocyanin-labeled anti-CD25 (PC61). They were further sorted on a FACSAria cell sorter (BD Biosciences) to obtain pure populations of CD4+CD25-CD62L^{hi} naïve T cells and CD4+CD25+ natural regulatory T cells (Treg). Naïve CD4+CD25-CD62L^{hi} cells were then incubated on anti–CD3-coated plastic plates (2 μg/mL) in complete RPMI 1640 with soluble anti-CD28 (2 μg/mL) and rTGF-β1 (1 ng/mL) to induce Foxp3+ Tregs. CD4+CD25+ natural Tregs were stimulated with anti-CD3–coated plastic plates (2 μg/mL) and soluble anti-CD28 (2 μg/mL). The cultures were supplemented with WP1066 at concentrations of 0, 0.1, and 1.0 μmol/L, respectively. Peridinin-chlorophyll-protein complex–conjugated anti-CD4 (L3T4) and allophycocyanin-conjugated anti-CD25 (PC61) monoclonal antibodies were used for cell surface staining. To detect FoxP3 protein expression, the surface-stained cells were further subjected to intracellular staining with phycoerythrin-conjugated monoclonal antibodies to mouse FoxP3 (clone FJK-16s; eBioscience) using staining buffers and conditions specified by the manufacturer.

Treg detection in human melanoma brain metastases and peritumoral CNS tissue. Fresh human tumors and peritumoral tissue were obtained from patients undergoing surgical resection for melanoma metastasis to the brain. The tumor and peritumoral tissue was identified and separated by an experienced neurosurgeon (A.B.H.) before submission to the laboratory. The analysis of the tissue was conducted under protocol # LAB03-0687, which was approved by the institutional review board at M. D. Anderson, and informed consent was obtained. Tissues were transported on ice from the operating room and were mechanically dissociated in the laboratory. Red cell lysing buffer was added to the cell suspensions before washing them with PBS. Cells were transferred to a 96-well culture plate and stained for surface markers using human allophycocyanin-labeled anti-CD4 and phycoerythrin-labeled anti-CD25 antibodies (BD Biosciences). Cells were then fixed and made permeable before intracellular FoxP3 staining with human FITC-labeled anti-FoxP3 (eBioscience) as described previously (24).

Statistical analysis. Kaplan-Meier product-limit survival probability estimates of overall survival were calculated (25), and log-rank tests (26) were done to compare overall survival between treatment groups and the control arm. For the tumor growth data set, at each time point when the mice were measured, since 2 cages of mice used either for treatment arm or for control arm, respectively, the nested two-factor model was used to assess the effect of drug treatment and cage by the formula: $y_{ijk} = u. + \alpha_i + \beta_{j(i)} + \varepsilon_{ijk}$ where $i = 1, 2$ (treatment and control arm); $j = 1, 2$ (cage); and k is the indicator of mice within cage (arm) combination. The difference in mean tumor growth between the treatment and control arms (α_i) was compared. For all the repeated tumor measurements of mice over time, the mixed model was used (27) and assessed by the formula: $y_{ijk} = u + \alpha_i + d_{ij} + \tau_k + (\alpha\tau)_{ik} + \varepsilon_{ijk}$ where $i = 1, 2$ (treatment and control arm); j is the indicator of mice within cage (arm) combination; and k = time k for tumor measurement; where d_{ij} and ε_{ijk} are normally independently distributed (NID) with $d_{ij} \sim NID\ (0, \sigma 2s)$ and $\varepsilon_{ijk} \sim NID\ (0, \sigma^2_\varepsilon)$. A P value of

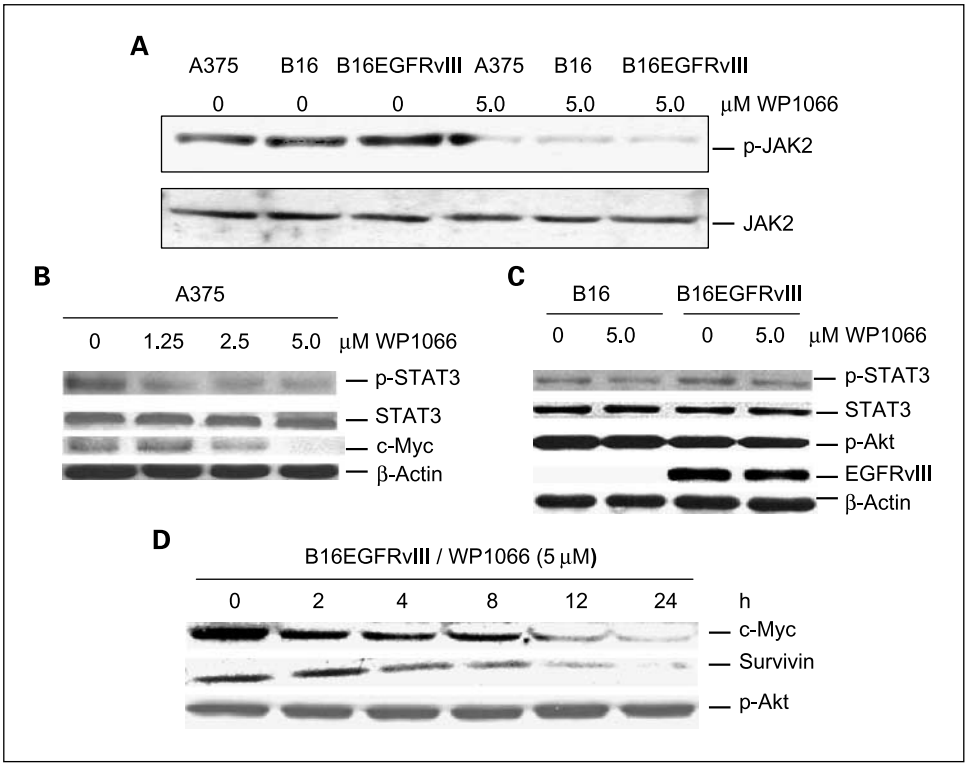

Fig. 1. Western blot analyses showing that WP1066 suppresses the intracellular signaling of p-JAK2, p-STAT3, c-Myc, and survivin in melanoma cells. *A,* A375, B16, or B16EGFRvIII cells were cultured with either medium alone or medium supplemented with 5 μmol/L of WP1066 for 2 h. Cell lysates were prepared and quantified for protein content. A total of 40 μg protein from each sample was used for immunoprecipitation and immunoblotting analysis of phospho-JAK2. Antiphosphotyrosine 4G10 conjugated to agarose beads was used for immunoprecipitation, and anti-JAK2 antibody was used for Western blotting. *B,* A375 cells were incubated with WP1066 at concentrations of 0, 1.25, 2.5, and 5 μmol/L for 2 h. *C,* B16 or B16EGFRvIII cells were cultured with either medium alone or medium supplemented with 5 μmol/L of WP1066 for 2 h. *D,* B16EGFRvIII cells were cultured with 5 μmol/L of WP1066 for 0, 2, 4, 8, 12, and 24 h. A total of 20 μg protein was electrophoretically fractionated in 8% SDS-polyacrylamide gels, transferred to nitrocellulose membranes, and followed by immunoblot analysis with specific antibodies against phospho-STAT3 (Tyr705), total STAT3, c-Myc, survivin, and β-Actin. In addition, the transferred membranes from B16 and B16EGFRvIII cell lysates were immunoblotted with a specific antibody against phospho-Akt (Ser473) or EGFRvIII.

≤0.05 was considered statistically significant. The *in vitro* cytotoxicity was analyzed using the unpaired standard Student's *t* test.

Results

Toxicity. To define the maximum tolerated dose, a single titered dose of WP1066 was administered i.p. to mice with severe combined immunodeficiency mice. At a dose of 120 mg/kg, symptoms of acute toxicity included diarrhea and a high frequency of urination. Chronic toxicity (at 3 months), including adhesion of the mouse intestine to the abdominal wall and muscle and death was observed in 1 of 5 mice. Further escalation of the dose to 140 mg/kg resulted in the death of 3 of 5 mice in the same interval. Neither acute nor chronic toxicity was observed in the vehicle (control) group. When injections of 50 mg/kg were delivered once per day for 5 days (with a rest for 2 days) for a total of 2 weeks, acute toxicity was observed in 1 of 8 mice, and chronic toxicity was observed in 2 of 8 in the treated group; thus, 40 mg/kg once per day, 5 times per week was selected as the maximal dose of WP1066, in which severe combined immunodeficiency mice did not have either acute or chronic toxicity. Within immune competent C57BL/6J mice, the maximum tolerated dose of WP1066 delivered i.p. was 20 mg/kg. When the dose of 40 mg/kg was delivered by tail vein injection in mice every other day for a total of five injections, there was marked inflammation and sclerosis of the vessel. In contrast, when doses of up to 120 mg/kg were administered every other day by o.g. for 8 doses and 180 mg/kg for 5 doses, no acute or chronic toxicity symptoms were observed. An maximum tolerated dose for o.g. in C57BL/6J mice could not be established above 40 mg/kg.

The spleens, kidneys, lungs, hearts, and brains of C57BL/6J mice treated with WP1066 underwent a detailed histologic examination by a pathologist blinded to the treatment group. No significant abnormalities were found in these mice (Table 1). Because WP1066 is an immune activator, nonspecific immune reactivity remains a consideration. Therefore, Luxol fast blue staining was conducted on the CNS axis to determine if there was evidence of induction of autoimmunity. No focal plaques of demyelination or significant macrophage infiltration were observed in areas without tumor in any animal treated with WP1066.

***WP1066 inhibits growth of melanoma cell lines* in vitro.** To determine if there was a direct cytostatic effect of WP1066 on the growth of B16, B16EGFRvIII, or A375 cells, these cell lines (in logarithmic growth) were exposed to WP1066 at concentrations of 0, 0.155, 0.3125, 0.625, 1.25, 2.5, 5.0, and 10 μmol/L. After 72 h, the dimethyl thiazolyl diphenyl tetrazolium salt assay was done; the IC_{50s} for B16, B16EGFRvIII, and A375 cells were 2.3, 1.5, and 1.6 μmol/L of WP1066, respectively.

WP1066 suppresses phosphorylation of JAK2 and STAT3. To determine on which pathways WP1066 exerts its activity, molecules both upstream and downstream of the STAT3 pathway were evaluated by Western blot analysis. WP1066 inhibited the phosphorylation of JAK2 in all three melanoma cell lines tested (Fig. 1A). In human melanoma cell line A375, WP1066 inhibited the phosphorylation of STAT3 and decreased the level of c-Myc in a dose-dependent manner (Fig. 1B). The inhibition of phosphorylated STAT3 (p-STAT3) by WP1066 in the murine melanoma cell lines B16 and B16EGFRvIII seemed weaker than for A375 cells (Fig. 1C). When the B16 melanoma line was stably transfected with the murine equivalent of EGFRvIII, which is the constitutively active variant of EGFR, overall, STAT3 did not seem to be appreciably up-regulated (Fig. 1C). In the B16EGFRvIII cell line, WP1066 did not affect p-Akt of the JAK/PI3K/AKT/mammalian target of rapamycin pathway, but it decreased the level of c-Myc and survivin in a time-dependent manner (Fig. 1D).

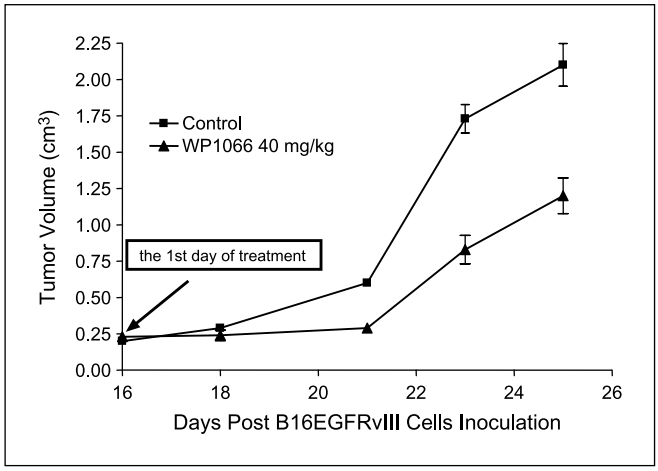

Fig. 2. Volume of subcutaneous B16EGFRvIII tumors in C57BL/6J mice treated with vehicle control or with WP1066 via o.g. once per day after tumors were measurable ($n = 6$ per group per experiment). On day 25, a P value of < 0.05 comparing the WP1066-treated group to the vehicle control-treated group. The figure is the result of a single experiment, but repeated twice.

Treatment with WP1066 suppresses the growth of subcutaneous melanoma. To determine whether treatment with WP1066 would retard the formation of subcutaneous tumors in a syngeneic system, C57BL/6J mice were injected with B16EGFRvIII cells and then treated on day 16 with WP1066, when tumors were grossly evident. Subcutaneous tumor growth progressed in all of the C57BL/6J mice treated with the vehicle control. For example, in one experiment, the mean cross-sectional areas of the tumors in the control group on days 18, 20, 23, and 25 were 169 ± 71, 352 ± 149, 980 ± 309, and 1,294 ± 621 mm^2, respectively. In contrast, in the WP1066-treated group, the mean cross-sectional areas were 100 ± 54 mm^2 ($P = 0.04$; compared with the control group), 155 ± 102 mm^2 ($P = 0.004$), 441 ± 334 mm^2 ($P = 0.01$), and 666 ± 562 mm^2 ($P = 0.05$; Fig. 2). These data were similar in two separate experiments. WP1066 also significantly inhibited tumor growth in nude mice injected with subcutaneous A375 cells in two independent experiments (data not shown).

WP1066 is efficacious in the treatment of C57BL/6J mice with established intracerebral tumors. To determine whether treatment was also efficacious against established intracerebral tumors, C57BL/6J mice with intracerebral tumors from B16EGFRvIII cells were treated with WP1066 (i.p and o.g.) starting on day 3 after tumor cell implantation. The median survival time for the control group was 17.5 days (95% confidence interval; 16, NA). For mice treated i.p. with 10 ($n = 10$) and 20 ($n = 10$) mg/kg of WP1066, the median survival times were 18.5 days (95% confidence interval; 17, NA) and 23.5 days (95% confidence interval; 19, NA), respectively. This

was statistically significant ($P < 0.001$) for mice treated with WP1066 at the 20 mg/kg dose (Fig. 3A). For the mice treated by o.g. with WP1066 at 40 mg/kg ($n = 10$), 80% survived long term (>78 days; $P < 0.0001$ compared with the control group), and there was at least a 324% increase in median survival time when the experiment was terminated to perform the tumor rechallenge experiments (Fig. 3B). Similar data and results were obtained for the mice with established intracerebral B16 tumors treated with WP1066 (Fig. 3C).

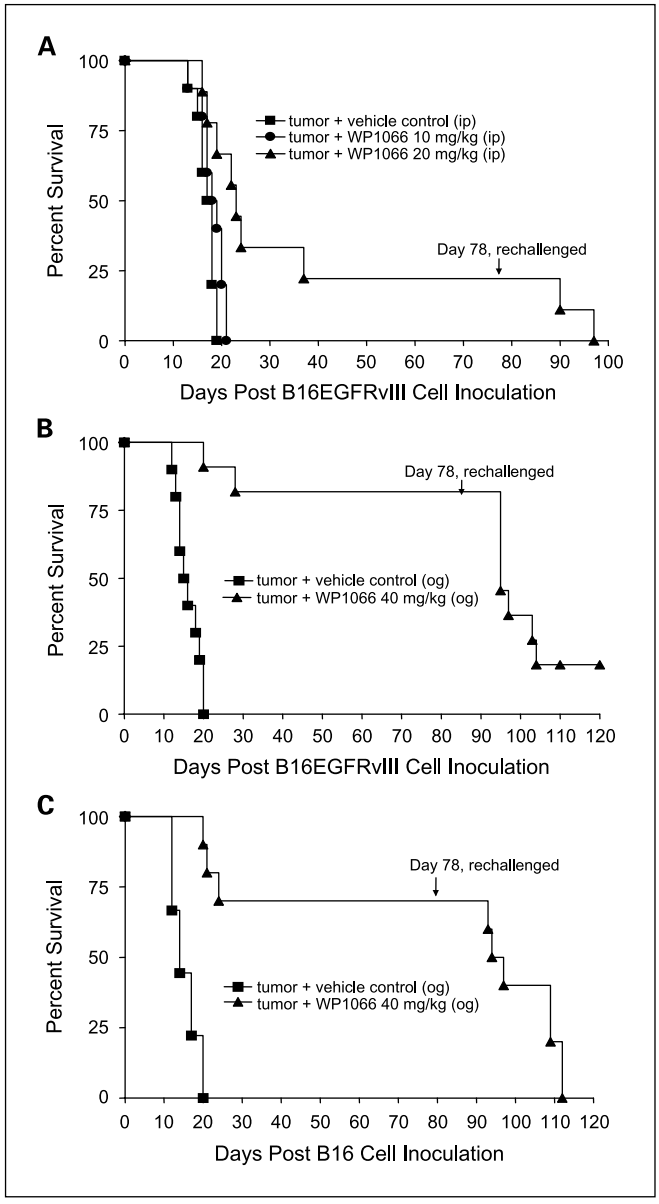

Fig. 3. Survival data from C57BL/6J mice treated with WP1066 after intracerebral B16EGFRvIII cells or B16 cells were established in the brain. *A,* antitumor efficacy was observed in mice injected i.p. with WP1066 ($n = 10$ per dose), but it was dose limiting owing to localized inflammation. A comparison of survival time in the group treated i.p. with WP1066 at 20 mg/kg with that for the vehicle control group yielded *P* values of 0.027, 0.011, 0.005, 0.002, and 0.001 on days 30, 35, 40, 45, and 50, respectively. *B,* C57BL/6J mice with established intracerebral B16EGFRvIII cells treated with WP1066 via o.g. ($n = 10$) showed at least a 324% increase in their median survival time, and 80% achieved long-term survival compared with those in the vehicle-treated controls ($n = 10$). For the group treated with 40 mg/kg WP1066 by o.g., the *P* values were 0.04, 0.18, 0.007, 0.002, 0.001, and 0.001 at days 25, 30. 35, 40, 45, and 50, respectively, compared with the vehicle control group. *C,* antitumor efficacy was also observed in C57BL/6J mice with established intracerebral B16 cells treated with WP1066 via o.g. ($n = 10$). In animals that survived longer than 78 d, subsequent rechallenge by injection of tumor cells into the contralateral hemisphere indicated that minimal immunologic memory was induced (*A-C*).

Mice treated with WP1066 do not develop immunologic memory. To determine if mice with intracerebral tumors treated with WP1066 were able to generate long-lasting protection against tumor regrowth, mice that survived for 78 days after the initial tumor cell implantation were reinoculated with B16EGFRvIII cells but in the contralateral hemisphere. Upon this rechallenge, in the animal group that had received WP1066 via o.g., the median survival time was 18 days (95% confidence interval; 17, NA), which was significantly different from 11 days, the median survival time of naïve animals challenged at the same time (95% confidence interval; 10, NA; $P < 0.001$); however, only 10% of the mice were long-term survivors (Fig. 3B). Similar data and results were obtained in the survival of mice with intracerebral B16 tumors (Fig. 3C).

WP1066 inhibits the production of immunosuppressive cytokines in melanoma cell lines. To determine if WP1066 could exert an effect on the immunosuppressive and proangiogenic properties of melanoma, B16 and B16EGFRvIII cells were treated for 24 hours with doses of WP1066 below the IC_{50}, the supernatant was harvested, and the cytokine production was determined by ELISA. Inhibition of TGF-β, the regulated on activation normal T-expressed and secreted (RANTES) cytokine, VEGF, and the Treg chemotaxic cytokine, MCP-1, were noted starting at a dose of 0.01 μmol/L of WP1066 (Fig. 4).

Vaccination with WP1066 does not enhance humoral immunity. To determine whether WP1066 enhanced humoral responses, C57BL/6J mice vaccinated with PBS, WP1066, PEP-3-KLH, PEP-3-KLH + WP1066, and PEP-3-KLH + CFA were examined for humoral responses after the first and third vaccinations. None of the animals treated with PBS ($n = 3$), PEP-3-KLH ($n = 3$), or PEP-3-KLH + CFA ($n = 3$) had detectable humoral responses to EGFRvIII after the first vaccination. EGFRvIII humoral responses were not detected in the mice that were vaccinated thrice with PBS ($n = 5$), PEP-3-KLH ($n = 5$), or WP1066 alone ($n = 4$). As expected, mice that were vaccinated thrice with PEP-3-KLH + CFA ($n = 5$) produced significant quantities of IgG antibody, ranging from 1,156 to 10,308 ng/mL. In contrast, mice treated with the combination of PEP-3-KLH + WP1066 ($n = 5$) showed no detectable EGFRvIII antibody responses. Furthermore, in animals ($n = 8$) that survived intracerebral tumor treatment with WP1066, none showed the induction of EGFRvIII-specific responses (Fig. 5A).

Vaccination with WP1066 induces T-cell cytotoxic responses. To determine whether WP1066 enhanced cytotoxic responses directed against PEP-3, splenocytes from naïve C57BL/6J mice and C57BL/6J mice vaccinated with PEP-3-KLH, WP1066, PEP-3-KLH + WP1066, and PEP-3-KLH + CFA were stimulated *in vitro* with B16EGFRvIII cells, and cytotoxicity was assessed against carboxyfluorescein succinimidyl ester–labeled B16EGFRvIII target cells. The naïve mice showed minimal lysis of the B16EGFRvIII target cells. The PEP-3-KLH– or WP1066-treated mice had increased cytotoxic clearance of the B16EGFRvIII target cells compared with naïve mice (Fig. 5B). In mice treated with both PEP-3-KLH and WP1066, there was further significant enhanced cytotoxic clearance of the B16EGFRvIII

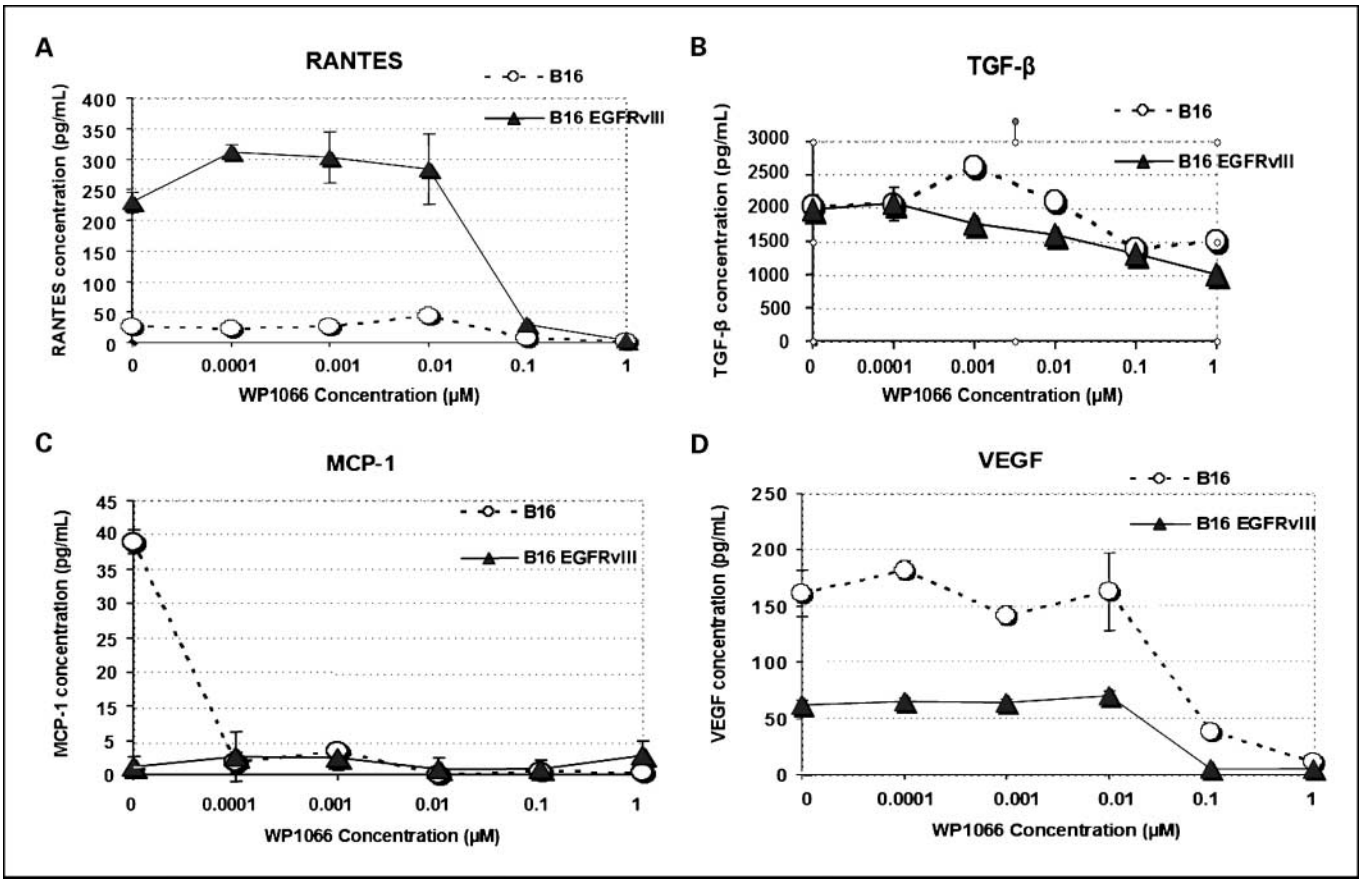

Fig. 4. The production of TGF-β, MCP-1, RANTES, and VEGF is inhibited by WP1066 at doses below the IC_{50}. B16 and B16EGFRvIII cells in logarithmic growth were treated with titered doses of WP1066 for 24 h. At a dose of 0.01 μmol/L WP1066, the cytokines TGF-β, RANTES, VEGF, and the Treg chemokine MCP-1 were all inhibited, as detected in ELISA assays.

target cells compared with mice that were treated with either WP1066 or PEP-3-KLH alone ($P < 0.05$; Fig. 5B).

WP1066 inhibits FoxP3 induction in peripheral T cells and down-regulates FoxP3 in natural Tregs. To investigate the effects of WP1066 on the peripheral induction of FoxP3+ Tregs, we used an *in vitro* Treg induction system in which FoxP3 expression was induced in naïve CD4+ ($CD4+CD25-CD62L^{hi}$) T cells isolated from the spleens of C57BL/6J mice. FoxP3+ Treg generation was directly measured by intracellular staining for FoxP3 protein expression. In this system, naïve CD4+ T cells underwent robust FoxP3+ Treg differentiation when they were activated by polyclonal stimulation in the presence of exogenous TGF-β. In contrast, WP1066 inhibited FoxP3+ Treg induction, compared with the control, from 70% to 54% at a 1.0 μmol/L concentration of WP1066 (Fig. 5C). Moreover, 1.0 μmol/L of WP1066 reduced Foxp3+ natural Tregs to 13.8% under polyclonal stimulation (Fig. 5C). Thus, WP1066 can diminish the induction of Tregs, which may contribute to the antitumor responses observed with its use *in vivo*.

Treg cells are present in both tumor and peritumoral tissue of patients with melanoma metastasis to the brain. To determine if Tregs were present within human melanoma in the CNS, we dissected the peritumoral brain tissue from the metastatic tumor, dissociated each respectively into a single-cell suspension, and then stained for the presence of CD4+CD25+FoxP3+ cells by flow cytometric analysis as we have previously described (24). Both peritumoral brain isolated 1 cm from the tumor margin and the melanoma metastasis contained CD4+CD25+FoxP3+ Tregs, with greater numbers located within the metastasis (Fig. 5D).

Discussion

We have designed and synthesized WP1066, an inhibitor of the JAK2/STAT3 pathway, which showed marked *in vivo* efficacy for treating established intracerebral syngeneic melanoma. The oral administration route showed optimal efficacy and minimal toxicity *in vivo*, which is desirable for continued development and translation to human subjects. Although efficacy was observed with i.p. or i.v. dosing, these administration routes were limited owing to localized inflammatory responses, specifically, peritoneal adhesions and venous sclerosis. The assessment of systemic organs from mice that received WP1066 failed to show other significant toxicities, but more specifically and most importantly, Luxol fast blue staining of the CNS failed to reveal evidence of demyelination or macrophage infiltration in areas of the CNS that did not harbor the intracerebral tumor that would indicate the inadvertent induction of autoimmunity. This is probably because STAT3 has been shown to be the key regulator for the generation of Th17 cells (28, 29), which are primary immune cell mediators

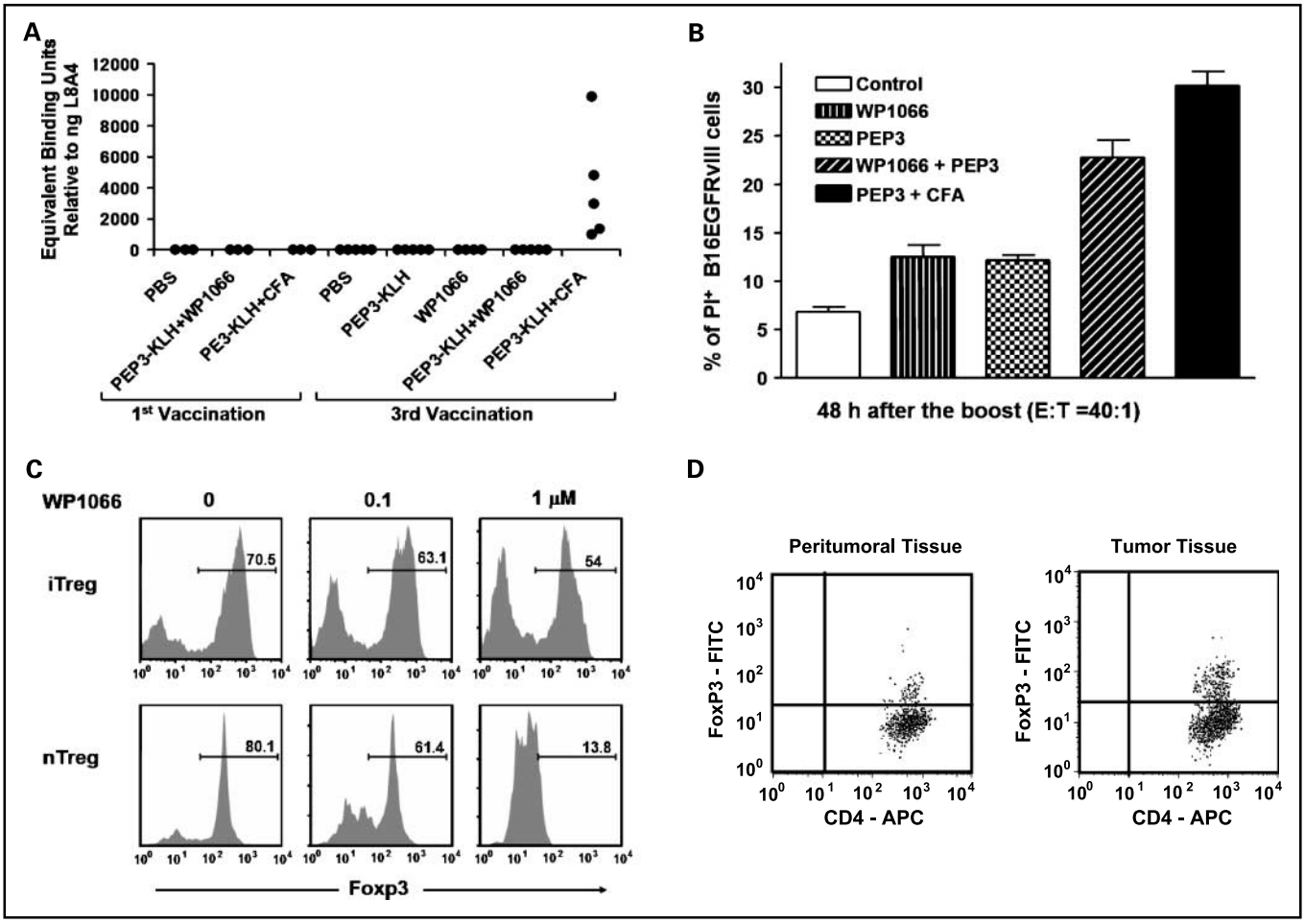

Fig. 5. *A,* humoral responses were not induced in mice vaccinated with PEP-3-KLH and WP1066 but were induced, as anticipated, with PEP-3-KLH and CFA. *B,* cytotoxicity of the B16EGFRvIII cells *in vitro* produced by splenocytes from mice vaccinated with PEP-3-KLH or with PEP-3-KLH plus WP1066. The splenocyte effector cells from mice that were vaccinated with PEP-3-KLH induced minimal lysis. However, splenocyte effector cells from mice that were vaccinated with PEP-3-KLH plus WP1066 potently enhanced EGFRvIII-specific lysis ($P < 0.05$). Columns, mean; bars, SD. *C,* WP1066 inhibits FoxP3 induction in T cells in peripheral blood and down-regulates FoxP3 in natural Tregs. CD4+CD25-CD62Lhi naïve T cells from C57BL/6J mice were stimulated by plate-bound anti-CD3 (2 ug/mL) and soluble anti-CD28 (2 ug/mL) in the presence of TGFβ1 (1 ng/mL) and hIL2 (200 U/mL) with 0, 0.1, and 1.0 mmol/L WP1066 for inducible Tregs (*iTreg*) differentiation; CD4+CD25+ T cells (*nTreg,* natural Tregs) were stimulated by plate-bound anti-CD3 (2 ug/mL) and soluble anti-CD28 (2 ug/mL) in the presence of hIL2 (200 U/mL) with 0, 0.1, and 1.0 mmol/L WP1066. Ninety-six hours after stimulation, the cells were analyzed for intracellular FoxP3 expression by flow cytometry. The percentage numbers for the indicated population are shown. *D*, fluorescence-activated cell sorting staining of peritumoral and tumor tissue isolated from a patient with melanoma metastasis to the brain. CD4+ cells were gated from the total cell population and plotted against FoxP3.

of autoimmunity (30). Thus, WP1066, an inhibitor of the STAT3 pathway that has been shown to markedly inhibit p-STAT3 within immune cells (19), should theoretically inhibit both TH17 cell generation and production of Tregs.

In this report, we show that WP1066 markedly inhibited both natural and inducible Treg proliferation, and this may account partially for the antitumor effects we observed *in vivo* and the enhancement of cytotoxic T-cell response. Previous studies in mice have shown that the ablation of Stat3 in the hematopoietic system using the Mx1-Cre-loxP system was accompanied by a reduction in the number of tumor-infiltrating Tregs (31). STAT3 has been shown to be required for both TGF-β and interleukin 10 production by CD4+ T cells (32), factors necessary for the generation of tumor-associated Tregs. Interleukin 2 has been shown to regulate FoxP3 expression in human CD4+CD25+ Tregs by STAT3 binding of the first intron of the *FoxP3* gene (33). The suppressor of cytokine signaling-3 has been shown to inhibit STAT3 signaling (34) and transcriptional activity (35, 36) but is deficient in Tregs (37). The effect and mechanism of WP1066 on the induction of Tregs is different from other known Treg modulatory agents such as anti-CD25, which binds to the surface of Tregs and disrupts the functional activity (38), and anti-CTLA4, which confers resistance to Treg-mediated suppression but not through a direct effect on Tregs (39). A metronomic cyclophosphamide regimen has been shown to selectively deplete numbers of Tregs (40), but it is not known if this occurs via the STAT3 pathway. Regardless, these other Treg modulators, at the doses administered, lack the significant intrinsic direct tumor cytotoxicity properties possessed by WP1066. Because Tregs are present within CNS melanoma, the inhibitory effect of WP1066 on Tregs has clinical implications, especially considering that immunotherapeutic approaches for melanoma have been disappointing (20). WP1066 could potentially be used in combination with other immunotherapeutic approaches such as dendritic cells (41),

peptide vaccination (21), or cytokine immunotherapy, such as interleukin 2 or IFN.

In addition to immune modulatory properties, WP1066 also acts directly upon the process of tumorgenesis and metastasis by inhibiting the phosphorylation of STAT3 and the subsequent downstream molecules, such as survivin and c-Myc. For human melanoma, unregulated c-Myc protein has also been correlated with poor clinical outcome in both primary and secondary diseases (42, 43), and RANTES has been shown to enhance tumor formation (44). The inhibition of multiple tumorigenic signaling pathways is highly desirable because of the heterogeneity of cancers and the redundancy of cancer growth signaling pathways. In the case of the B16 tumor cell line, the changes in p-STAT3 levels were subtle after treatment with WP1066. This could be because the Western blot analysis was conducted on whole cell lysates, possibly causing changes in nuclear p-STAT3 to go undetected. Alternatively, the 2 hours of WP1066 treatment may not have been an optimal time for assessing p-STAT3 levels. Most likely, a key mechanism in the efficacy of WP1066 is its activity upon other cells within the tumor microenvironment, such as T- and natural killer cells (31, 45) and the cells or factors that support or propagate angiogenesis, such as VEGF.

Patients with advanced malignancies are profoundly immunosuppressed, and even if a systemic immune response could be generated, it could be negated within the tumor microenvironment by a wide variety of factors, such as Tregs (24, 46, 47), immunosuppressive cytokines, and immunosuppressive macrophages (24). We have recently shown that WP1066 can modulate this tumor microenvironment, specifically by increasing costimulatory molecule expression on immunosuppressive macrophages/microglia (19). Here, we have shown that WP1066 can also inhibit the elaboration of immunosuppressive cytokines such as TGF-β and the Treg chemokine MCP-1 (48) below the IC_{50}, indicating that WP1066 has tumor microenvironment modulatory properties that could overcome some of these immunologic barriers in patients with solid malignancies.

In mice previously treated with WP1066 who were rechallenged with tumor cell inoculation, the longer median survival time compared with naïve control animals showed a partial protective immune effect. Yet, ultimately, these mice were not long-term survivors, indicating that maintenance of the immune effects of WP1066 will require sustained dosing if a tumor recurs. Although WP1066 did not seem to enhance humoral responses or induce immunologic memory that is fully protective for tumor rechallenge, WP1066 inhibits immunosuppressive cytokines, enhances costimulatory molecule expression within the tumor microenvironment (19), enhances cytotoxic T-cell responses, and inhibits the induction of Tregs. Given its oral bioavailability, inherent immunomodulatory properties, direct tumor cytotoxicity activity, ability to enter the CNS, and efficacy against established CNS tumors, WP1066 is a compelling agent for further development and translation to applications for patients with intracerebral melanoma metastasis—a major unmet clinical need. Marked anticancer activity of WP1066 has also been shown against head and neck carcinoma (13), pancreatic cancer (49), bladder cancer (11), gliomas (12), B-cell non–Hodgkin's lymphoma and myeloma (14), and chronic myelogenous leukemia (50), indicating that this class of compounds has broad potential for treatment of oncological disease.

Disclosure of Potential Conflicts of Interest

No potential conflicts of interest were disclosed.

Acknowledgments

We thank David M. Wildrick, PhD for editorial assistance.

References

1. Yu H, Jove R. The STATs of cancer-new molecular targets come of age. Nat Rev Cancer 2004;4:97–105.
2. Huang S. Regulation of metastases by signal transducer and activator of transcription 3 signaling pathway: clinical implications. Clin Cancer Res 2007;13:1362–6.
3. Xie TX, Wei D, Liu M, et al. Stat3 activation regulates the expression of matrix metalloproteinase-2 and tumor invasion and metastasis. Oncogene 2004;23:3550–60.
4. Lo HW, Hsu SC, Ali-Seyed M, et al. Nuclear interaction of EGFR and STAT3 in the activation of the iNOS/NO pathway. Cancer Cell 2005;7:575–89.
5. Haura EB, Zheng Z, Song L, Cantor A, Bepler G. Activated epidermal growth factor receptor-Stat-3 signaling promotes tumor survival *in vivo* in non-small cell lung cancer. Clin Cancer Res 2005;11:8288–94.
6. Mizoguchi M, Betensky RA, Batchelor TT, Bernay DC, Louis DN, Nutt CL. Activation of STAT3, MAPK, and AKT in malignant astrocytic gliomas: correlation with EGFR status, tumor grade, and survival. J Neuropathol Exp Neurol 2006;65:1181–8.
7. Alvarez JV, Greulich H, Sellers WR, Meyerson M, Frank DA. Signal transducer and activator of transcription 3 is required for the oncogenic effects of non-small-cell lung cancer-associated mutations of the epidermal growth factor receptor. Cancer Res 2006;66:3162–8.
8. Akca H, Tani M, Hishida T, Matsumoto S, Yokota J. Activation of the AKT and STAT3 pathways and prolonged survival by a mutant EGFR in human lung cancer cells. Lung Cancer 2006;54:25–33.
9. Ferrajoli A, Faderl S, Van Q, et al. WP1066 disrupts Janus kinase-2 and induces caspase-dependent apoptosis in acute myelogenous leukemia cells. Cancer Res 2007;67:11291–9.
10. Guha S, Chakraborty A, Szymanski S, et al. WP1066, a potent inhibitor of Jak2/STAT3 pathway inhibits pancreatic tumor growth both *in vitro* and *in vivo*. 98th American Association of Cancer Research Annual Meeting, Los Angeles, CA, 2007.
11. Chakraborty A, Guha S, Helgason T, et al. A novel Jak2/STAT3 pathway inhibitor promotes apoptosis and blocks growth of bladder cancer cells. 98th American Association of Cancer Research Annual Meeting, Los Angeles, CA, 2007.
12. Iwamaru A, Szymanski S, Iwado E, et al. A novel inhibitor of the STAT3 pathway induces apoptosis in malignant glioma cells both *in vitro* and *in vivo*. Oncogene 2006;26:2435–44.
13. Kupferman ME, Zhou G, Zhao M, et al. A novel inhibitor of STAT3 signaling in head and neck squamous cell carcinoma. 97th American Association of Cancer Research Annual Meeting, Washington, DC, 2006.
14. Kong L-Y, Kapuria V, Bartholomeusz G, Priebe W, Talpaz M, Donato N. Antitumor activity and mechanism of action of a novel Stat3 inhibitor, WP1066, against human B-cell non-Hodgkin's lymphoma and multiple myeloma. Blood. Vol. 106, 2005;429A,1489 Part 1.
15. Kong L-Y, Talpaz M, Priebe W, et al. Novel tyrphostin analogues inhibit Stat3 activation and induce apoptosis in multiple hematological malignancies. The 45th Annual Meeting of the American Society of Hematology San Diego, CA, 2003.
16. Donato NJ, Wu J, Kong L-Y, Meng F, Priebe W, Talpaz M. Targeting BCR-ABL and its downstream signaling cascade as therapy for chronic myelogenous leukemia. The 46th Annual Meeting of the American Society of Hematology, San Diego, CA, 2004.
17. Yu H, Kortylewski M, Pardoll D. Crosstalk between cancer and immune cells: role of STAT3 in the tumour microenvironment. Nat Rev Immunol 2007;7:41–51.
18. Kortylewski M, Yu H. Stat3 as a potential target for cancer immunotherapy. J Immunother (1997) 2007;30:131–9.
19. Hussain SF, Kong L-Y, Jordan J, et al. A novel small molecule inhibitor of signal transducers and activators of transcription 3 reverses immune tolerance in malignant glioma patients. Cancer Res 2007;67:9630–6.
20. Rosenberg SA, Yang JC, Restifo NP. Cancer immunotherapy: moving beyond current vaccines. Nat Med 2004;10:909–15.
21. Heimberger AB, Crotty LE, Archer GE, et al. Epidermal growth factor receptor VIII peptide vaccination is efficacious against established intracerebral tumors. Clin Cancer Res 2003;9:4247–54.
22. Coligan JE, Kruisbeck AM, Margulies DH, Shevach EM, Strober W. Current protocols in immunology. New York: Green & Wiley Interscience; 1994.

23. Heimberger AB, Sun W, Hussain SF, et al. Immunological responses in a patient with glioblastoma multiforme treated with sequential courses of temozolomide and immunotherapy: Case study. Neuro-oncol. E-pub 2007.

24. Hussain SF, Yang D, Suki D, Aldape K, Grimm E, Heimberger AB. The role of human glioma-infiltrating microglia/macrophages in mediating antitumor immune responses. Neuro-oncol 2006;8:261–79.

25. Kaplan EL, Meier P. Nonparametric estimation from incomplete observations. J Am Stat Assoc 1958;53:457–81.

26. Mantel N. Evaluation of survival data and two new rank order statistics arising in its consideration. Cancer Chemother Rep 1966;50:163–70.

27. Littell RC, Milliken GA, Stroup WW, Wolfinger RD. SAS system for mixed models. Cary (NC): SAS Institute Inc.; 1996.

28. Yang XO, Panopoulos AD, Nurieva R, et al. STAT3 regulates cytokine-mediated generation of inflammatory helper T cells. J Biol Chem 2007;282:9358–63.

29. Foley JF. STAT3 regulates the generation of Th17 cells. Sci STKE 2007;2007:tw113.

30. Bettelli E, Oukka M, Kuchroo VK. T(H)-17 cells in the circle of immunity and autoimmunity. Nat Immunol 2007;8:345–50.

31. Kortylewski M, Kujawski M, Wang T, et al. Inhibiting Stat3 signaling in the hematopoietic system elicits multicomponent antitumor immunity. Nat Med 2005;11:1314–21.

32. Kinjyo I, Inoue H, Hamano S, et al. Loss of SOCS3 in T helper cells resulted in reduced immune responses and hyperproduction of interleukin 10 and transforming growth factor-β1. J Exp Med 2006;203:1021–31.

33. Zorn E, Nelson EA, Mohseni M, et al. IL-2 regulates FOXP3 expression in human CD4+CD25+ regulatory T cells through a STAT-dependent mechanism and induces the expansion of these cells *in vivo*. Blood 2006;108:1571–9.

34. Yoshimura A, Naka T, Kubo M. SOCS proteins, cytokine signalling and immune regulation. Nat Rev Immunol 2007;7:454–65.

35. Starr R, Willson TA, Viney EM, et al. A family of cytokine-inducible inhibitors of signalling. Nature 1997;387:917–21.

36. Qin H, Roberts KL, Niyongere SA, Cong Y, Elson CO, Benveniste EN. Molecular mechanism of lipopolysaccharide-induced SOCS-3 gene expression in macrophages and microglia. J Immunol 2007;179:5966–76.

37. Pillemer BB, Xu H, Oriss TB, Qi Z, Ray A. Deficient SOCS3 expression in CD4+CD25+FoxP3+ regulatory T cells and SOCS3-mediated suppression of Treg function. Eur J Immunol 2007;37:2082–9.

38. Fecci PE, Sweeney AE, Grossi PM, et al. Systemic anti-CD25 monoclonal antibody administration safely enhances immunity in murine glioma without eliminating regulatory T cells. Clin Cancer Res 2006;12:4294–305.

39. Fecci PE, Ochiai H, Mitchell DA, et al. Systemic CTLA-4 blockade ameliorates glioma-induced changes to the CD4+ T cell compartment without affecting regulatory T-cell function. Clin Cancer Res 2007;13:2158–67.

40. Ghiringhelli F, Menard C, Puig PE, et al. Metronomic cyclophosphamide regimen selectively depletes CD4+CD25+ regulatory T cells and restores T and NK effector functions in end stage cancer patients. Cancer Immunol Immunother 2007;56:641–8.

41. Heimberger AB, Archer GE, Crotty LE, et al. Dendritic cells pulsed with a tumor-specific peptide induce long-lasting immunity and are effective against murine intracerebral melanoma. Neurosurgery 2002;50:158–64; discussion 64–6.

42. Kraehn GM, Utikal J, Udart M, et al. Extra c-myc oncogene copies in high risk cutaneous malignant melanoma and melanoma metastases. Br J Cancer 2001;84:72–9.

43. Chana JS, Grover R, Tulley P, et al. The c-myc oncogene: use of a biological prognostic marker as a potential target for gene therapy in melanoma. Br J Plast Surg 2002;55:623–7.

44. Mrowietz U, Schwenk U, Maune S, et al. The chemokine RANTES is secreted by human melanoma cells and is associated with enhanced tumour formation in nude mice. Br J Cancer 1999;79:1025–31.

45. Wang T, Niu G, Kortylewski M, et al. Regulation of the innate and adaptive immune responses by Stat-3 signaling in tumor cells. Nat Med 2004;10:48–54.

46. Fecci PE, Mitchell DA, Whitesides JF, et al. Increased regulatory T-cell fraction amidst a diminished CD4 compartment explains cellular immune defects in patients with malignant glioma. Cancer Res 2006;66:3294–302.

47. El Andaloussi A, Lesniak MS. CD4+ CD25+ FoxP3+ T-cell infiltration and heme oxygenase-1 expression correlate with tumor grade in human gliomas. J Neurooncol 2007;83:145–52.

48. Jordan JT, Sun WH, Hussain SF, DeAngulo G, Prabhu SS, Heimberger AB. Preferential migration of regulatory T cells mediated by glioma-secreted chemokines can be blocked with chemotherapy. Cancer Immunol Immunother 2008;57:123–31.

49. Bao JJ, Fokt I, Szymanski S, Priebe W. Inhibition of constitutively active STAT3 by WP1066 suppresses proliferation and induces apoptosis in pancreatic cancer cells. Clin Cancer Res 2005;11:9026–7S.

50. Samanta A, Kantarjian H, Priebe W, Arlinghaus R. Cross talk between Jak2 and Lyn in Bcr-Abl signaling pathway in cells from Imatinib-sensitive and resistant chronic myelogenous leukemia (CML). 98th American Association of Cancer Research Annual Meeting, Los Angeles, CA, 2007.